Ultra-high strength concrete on eccentrically loaded slender circular concrete-filled dual steel columns

C. Ibañez [a], M. L. Romero [b]*, A. Espinos [b], J.M. Portolés [a] and V. Albero [b]

*[a] Department of Mechanical Engineering and Construction,
Universitat Jaume I, Castellón, Spain*
*[b] Instituto de Ciencia y Tecnología del Hormigón (ICITECH),
Universitat Politècnica de València, Valencia, Spain*
* Corresponding author. e-mail address: mromero@mes.upv.es

ABSTRACT

This paper presents an experimental study which was undertaken to investigate the effect of ultra-high strength concrete (UHSC) on the mechanical response of concrete-filled dual steel tubular columns (CFDST) subjected to eccentric loads. This campaign is a continuation of a previous program on axially loaded members and consists in testing 12 CFDST specimens and two concrete-filled tubular (CFST) columns which serve as references. The location of the dual-grade concretes (outer ring and inner core) and the steel thicknesses configuration were the parameters analysed. Therefore, in this program, two series can be distinguished: 6 columns with normal strength concrete in their outer rings and, conversely, 6 with ultra-high strength concrete. In addition, two different steel tube thicknesses configurations were considered: columns with thin outer steel tube and thick steel tube (thin-thick); and the opposite pattern (thick-thin). Moreover, the experiments on the CFST columns of reference served to investigate the effect of the extra inner steel tube and its filling in CFDST columns. Since the number of campaigns on eccentrically loaded slender CFDST columns is scarce, the results presented in this work become particularly relevant. The analysis of the results revealed that, for both series, the response of the specimens showed similar trend but the effect of UHSC differed from that observed for axially loaded

columns. Finally, the experimental data were contrasted to the predictions given by Eurocode 4 for the design of composite columns resulting, in general, in slightly unsafe predictions.

Keywords: *Ultra-high strength concrete, concrete-filled steel tubular column, eccentric loads, concrete contribution ratio, double-tube, Eurocode 4.*

NOTATION

CHS	Circular hollow section
CFDST	Concrete-filled dual steel tubes
CFST	Concrete-filled steel tube
D	Diameter of the steel tube
t	thickness of the steel tube
e	eccentricity
$_{,ext}$	relating to the outer steel tube
$_{,int}$	relating to the inner steel tube
f_c	Compressive cylinder strength of concrete (test date)
f_y	Yield strength of structural steel
EC4	Eurocode 4
N_u	Ultimate axial load from tests
$N_{b,Rd}$	Design axial buckling load from EC4 Part 1-1
$\bar{\lambda}$	Relative slenderness

$$\bar{\lambda} = \sqrt{N_{pl} / N_{cr}} = \sqrt{(A_c f_c + A_a f_y + A_s f_s) / [(\pi^2 EI) / L^2]}$$

L	Column length

1. INTRODUCTION

In the last years, investigations on ultra-high strength concrete (UHSC) have acquired considerable relevance given its beneficial application in the building industry and the possibility to develop novel structural elements with improved mechanical behaviour.

In parallel, with the aim of enhancing the bearing capacity under compression loads, new configurations of concrete-filled steel tubular (CFST) columns have appeared focused on the main applications of these columns (high-rise buildings and bridge piers). Thus, a new innovative variant of CFST sections has been developed in which an extra inner tube is placed concentrically. These are named concrete-filled dual steel tubular (CFDST) columns and two types of cross-section configurations can be found as shown in Fig. 1: double-skin sections (Fig. 1a), where the inner core is empty, and double-tube sections (Fig. 1b), where the inner core is also filled with concrete.

One of the advantages of CFDST columns is the possibility of placing different grade concretes at the outer ring and inner core respectively so that it is feasible to find the best combination of concrete strengths for a specific structural response. In addition, the sectional steel tube thicknesses configuration is another parameter of study which can affect the efficiency of the concrete in the column given a certain load situation.

Thus, the employment of ultra-high strength concrete in CFDST columns, alone or combined with normal strength concrete, may help to increase considerably the bearing capacity of these composite columns with a reduced technological cost. In the case of CFST columns tested at ambient temperature, this effect was observed by Portolés et al. [1] through an extensive test program on slender columns, being the effect of UHSC as infill particularly significant for axially loaded columns.

3

Nevertheless, the usage of high strength materials may aggravate the buckling problems of CFST columns given the increment in the column slenderness produced by the diminution of the strictly needed net cross-sectional area. This can be especially important at higher temperatures where CFST columns have traditionally been appreciated by their good properties. Thus, replacing traditional CFST columns by CFDST columns with an inner steel tube which remains at a lower temperature in case of fire exposure may help to counteract second order effects and also spalling problems by placing UHSC in the inner steel tube.

With the purpose of characterizing CFDST columns, several experimental campaigns have been performed, most of them focused on stub columns with double-skin cross-section as published in [2]-[7]. In most of these works, the thick tube was placed outside and the thin tube at the inner part (thick-thin) [2] [5], although specimens with tubes with the same thickness were also tested. In all the columns, normal strength concrete was poured in the outer ring and the registered results were compared with the predictions given by Eurocode 4 Part 1-1 [8].

In the field of double-tube sections, where the inner tube is also filled with concrete, the work carried out by Liew and Xiong [9] on CFDST columns with CHS-CHS section is remarkable given the novelty of employing UHSC. A comparison of tests results with those provided by EC4-1-1 [8] showed a good agreement and safe predictions. However, once more all the specimens tested were stub columns so that second order effects could not be analysed.

In fact, the number of experimental works dealing with tests on slender columns is very limited in comparison with those on stub CFDST columns. Authors like Essopjee and Dundu [10] and Wan and Zha [11] reported experimental data on double-skin and double-tube slender columns under axial loads, although the influence of UHSC was not studied yet in these campaigns.

The same trend was initially followed by researchers on the area of single CFST columns. However, nowadays, several experimental programs on slender CFST columns subjected to eccentric loads can be found in the literature, such as one of the first campaigns performed by Rangan and Joyce [12] in the early nineties or the numerous works developed in the last decades (Han [13], Yu et al. [14], Lue et al. [15], Tao et al. [16], Portoles et al. [17]). Besides, some authors have also investigated the effect of double eccentricities on these slender columns such as Kilpatrick and Rangan [18] and Zeghiche and Chaoui [19] in circular, or Wang [20] and Hernández-Figueirido et al. [21][22] in rectangular CFST columns.

Given the lack of tests dealing with the characterization of the structural behaviour of slender CFDST columns with UHSC, also the authors developed an extensive experimental program where the columns were tested under axial loads [23][24] to analyse the effect of several parameters. Through this program it was proved the influence of placing UHSC in the outer ring being these specimens the ones resisting highest axial loads and where the combination of steel tube thicknesses had little influence.

Considering all, the necessity of more experimental campaigns on slender CFDST columns with UHSC still persists and this fact becomes even more relevant when refers to slender members subjected to eccentric loads. Moreover, the influence of the aforementioned second order effects may be even more remarkable with eccentric loads and for that reason an appropriate characterization of their behaviour is recommended.

Therefore, this paper presents the results of an experimental campaign on eccentrically loaded slender CFDST columns comprising the two variants previously described: double-skin and double-tube columns. Besides, the corresponding CFST columns of reference were tested for comparison purposes. The effect of the UHSC infill is studied and its location is varied to analyse the grade of influence of this parameter. Also, the position of the thick steel

tube was altered, leading to two different thicknesses configurations: outer steel tube thicker than the inner one (thick-thin) and the opposite one (thin-thick). The purpose of this work is to evaluate the structural behaviour of these configurations under eccentric loads and contrast the results with those obtained for axially loaded members in a previous campaign [24].

2. EXPERIMENTAL TESTS

2.1. General

In this paper, the results of a series of tests carried out on eccentrically loaded slender CFDST columns are presented. This campaign follows a previous batch of tests on axially loaded slender CFDST columns [24] started in the framework of an experimental program which will be, subsequently, completed with the corresponding tests under fire.

In this work, a total of 14 specimens were tested with the objective of evaluating the effect of three parameters: the effect of the concrete grade poured into the tubes (NSC and UHSC), the location of UHSC (inner core and outer ring) and the steel tubes thicknesses ratio.

Based on the previous tests on axially loaded members [24], the experiments subjected to eccentric loads were performed on the same collection of cross-section types for comparison purposes. Fig. 2 and Fig. 3 show the geometry of these specimens and the rest of details can be found in Table 1. According to the type of concrete placed in the outer ring, the columns can be divided into two different series of 6 specimens each: Series 3 with normal strength concrete of grade C30 (Fig. 2a) and Series 4 with ultra-high strength concrete of grade C150 (Fig. 2b). Note that the series in this campaign are named Series 3 and Series 4 according to the code employed in the framework of the general experimental program [24].

For the double-tube members of each series, the compressive strength of the concrete poured into the inner steel tube varied between C30 and C150 and in 4 of the specimens the inner steel tube was not filled (i.e. double-skin). The campaign was designed to assure that all

the columns had the same area of steel at the cross-section (with a maximum deviation of ±4%), taking as a reference the cross-section of a CFST column previously tested under fire by the group to facilitate future comparison of results (test C3 from [25]). The data describing the columns as well as the material tests results regarding the real compressive strengths are summarised in Table 1. Note that the identification of the CFDST specimens starts in NR13, being the first column included in this work the thirteenth column tested in the framework of the general experimental program at room temperature. Due to stock problems of the supplier, the specimens NR16-NR18 and NR22-NR24 had an outer diameter of 193.7 mm instead of 200 mm as the rest of columns. However, in any case this fact results in a distortion of the main conclusions that may be extracted from this experimental investigation.

For comparison purposes, two CFST columns (Fig. 2c) were tested as references. The columns had the same outer steel tube and were filled with normal strength concrete and ultra-high strength concrete respectively. In Table 1 their properties are included.

The study of the influence of the steel tubes thicknesses configuration on the mechanical response of the columns is one of the objectives fixed in this campaign. For axial loads, the authors observed that setting the thick tube at the outer part of the cross-section (thick-thin) enhanced the structural behaviour of these columns. Thus, it is essential to verify whether the same results are obtained also for eccentrically loaded CFDST columns in order to draw some design recommendations. Therefore, the thicknesses of the steel tubes are combined as shown in Table 1 so that 6 of the specimens had a thick inner tube and a thin outer tube (thin-thick) and the other 6 a thin inner tube and a thick outer tube (thick-thin).

2.2. Column specimens and test setup

All the columns were manufactured at Universitat Politècnica de València (Spain). A steel plate with dimensions 300x300x15 mm was welded at both ends of each column to

assure that the boundary conditions of the column during the tests were pinned-pinned (P-P) end conditions, resulting columns with a buckling length of 3315 mm.

However, the experiments were carried out at the laboratories of the Universitat Jaume I in Castellón (Spain) so that the same horizontal testing frame with capacity of 5000 kN used in the tests reported in [24] was employed. A schematic view of the test set-up including the testing frame and a column already positioned can be observed in Fig. 4. The axial load was applied with the same eccentricity at both ends with a value of 50 mm as displayed in Fig. 3c. As presented in Fig. 4, linear variable displacement transducers (LVDTs) were placed at five points along the column (0.25L, 0.375L, 0.5L, 0.625L and 0.75L) with the aim of measuring the deflection. As part of the preparation of the experiment, the pertinent displacement control test was executed after the correct positioning of the specimen in order to guarantee the proper measurement of the post-peak behaviour.

As shown schematically in Fig. 4, the strains were measured at the central cross-section using electrical strain gauges which recorded the deformation in the longitudinal direction at two locations, 0º and 180º, of both the inner and the outer steel tubes.

2.3. Material properties

Steel tubes

For all the hollow steel tubes employed in this experimental program, the actual values of the yield strength (f_y) were determined through the corresponding coupon tests (3 tests per tube) and are shown in Table 1. Owing to the available stock of the provider, the nominal yield strength of the steel tubes varied between S355 and S275. According to the European standards, the modulus of elasticity of steel was set to 210 GPa. In Fig. 2, the different CFDST columns tested can be observed, where both the inner tube and the outer tube are circular steel hollow sections (CHS-CHS).

8

Concrete

Regarding the concrete infill, two types of nominal compressive strength were employed: 30 MPa and 150 MPa whose mix proportions are summarized in Table 2 for each batch respectively. Together with the experiment on the slender CFDST column, the corresponding tests were carried out on both the 150x300 mm cylinder and the 100 mm cube in order to obtain the actual compressive strength (f_c) which characterizes each concrete infill of the column as shown in Table 1. For that task, sets of concrete samples were prepared in a planetary mixer and cured in standard conditions during 28 days.

3. RESULTS

3.1. Force-displacement

In Fig. 5 and Fig. 6 the different curves extracted from the experiments are displayed for the two series studied. During the tests, the evolution of the axial force and the lateral displacement at mid-span were registered for each column. For comparison, the behavior of the corresponding CFST columns of reference is also plotted. In Table 3 the value of the maximum axial load achieved for each column (N_u) is summarized, including also the results of the reference tests (i.e. CFST3 for Series 3 and CFST4 for Series 4).

In view of the results shown in Fig. 5, Fig. 6 and Table 3, it is found that under eccentric loads, none of the studied combinations of CFDST columns improves the load bearing capacity of the corresponding CFST of reference. This result was as expected, because in tests under eccentric loads the steel tube plays a more important role in counteracting the tensile stresses arising at the cross section. Moreover, this response was the opposite of that observed for the corresponding tests under axial loads, where the enhancement of the mechanical behavior of the CFDST columns with respect to the single CFST was the trend detected [24].

This can be observed in Fig. 7 where, as an example, the behavior of specimens from Series 4 are compared with that obtained for Series 2 from [24] which comprises the same specimens tested under axial loads.

Series 3: NSC in the outer ring

As displayed in Fig. 5, the specimens with the thin-thick combination have lower values of maximum load than the columns with the thick–thin configuration. The maximum load achieved increases with the compressive strength of the concrete in the inner tube. The specimen NR15, with the inner steel tube filled with UHSC, is the one showing the maximum load, although it is still less than that measured for the CFST of reference (CFST3).

For the thick-thin combination, as expected, the maximum load observed for the double-skin specimen is the lowest. In this case, the results again do follow a logical trend being the double-tube specimen with UHSC the one with the highest maximum load, which is very similar but still smaller (1037 kN and 1053 kN respectively) than that observed for the corresponding CFST column (CFST3).

In this series, the steel tubes configuration limits the influence of the UHSC infill and, in general, the effect of any type of concrete filling the inner core. Under eccentric loads, the cross-sectional stress distribution results in an important portion of the outer cross-sectional region working under tension. Thus, those specimens which present more steel area placed at the outer part (and consequently less concrete) are more efficient in this situation allowing a greater contribution of the inner concrete core to the total bearing capacity of the section.

Series 4: UHSC in the outer ring

In general, the maximum loads registered for the specimens of this series are higher than those corresponding to Series 3, being the columns with the combination thick-thin those showing the highest values.

10

In the view of the results displayed in Fig. 6, for both configurations of steel tubes, the increment in the maximum load detected between the double-skin and the double-tube specimens (NR19 versus NR20 and NR21; and NR22 versus NR23 and N24) is more notable than the increase experimented by the double-tube columns when the grade of the concrete infill varies. In these cases, the values of the maximum load are concentrated in a very narrow margin: 1311 kN and 1319 kN for the specimens NR20 and NR21 (thin-thick) and 1414 kN and 1419 kN for the specimens NR23 and NR24 (thick-thin), as can be observed in Table 3. Again, although slightly smaller, the specimen of the configuration thick-thin with the inner core filled with UHSC (NR24) is the one showing a maximum load similar to that of the corresponding CFST of reference (CFST4, Table 3).

The effect of the steel tubes configuration is noticeable, oppositely to the response shown by the tested axially loaded columns [24], where this effect was insignificant. This contrast can be observed in Fig. 7, where Series 2 from [24] is plotted together with Series 4 in order to show the different trends of these specimens under axial and eccentric loads respectively. For Series 2, the authors observed that the UHSC outer ring controlled the general behavior of the columns [24]. However, for the columns under eccentric loads, the effect of the UHSC ring is less pronounced given the important part of the outer region working under tension. Thus, the response of those specimens with the thick tube set at the outer part is enhanced since a larger area of steel can contribute to a major extend to counteract the tension stresses generated under eccentric loads.

3.2. Failure mode

It was found that the typical failure mode for all the tested specimens was the overall buckling mode. In Fig. 8, the longitudinal deformation of both steel tubes, inner and outer, is shown. Deformation at two different points of the central cross-section were measured: on the compression side (0°) and on the tension side (180°). For the sake of clarity, the deformations

11

obtained with the strain gauges have been grouped for each one of the steel tube thicknesses combinations which are included in each series. In general, it can be observed that both the tension and the compression strains are within the same order of magnitude. This indicates the proximity of the neutral axis to the centre of the cross-section so that an important part of the section is working under tension. In this situation, the concrete area becomes determinant in the ultimate failure load.

In the case of Series 3, where the columns have NSC concrete in the outer ring (Fig. 8a and b), the behaviour is more ductile than in the case of Series 4, with HSC in the outer ring (Fig. 8c and d). This loss of ductility can be observed in the slope of the post-peak curve, which is more abrupt and less smooth for Series 4.

In these graphs, also the marked influence of the infill in the inner steel tube in the case of Series 3 can be observed, contrarily to Series 4, where it is more noticeable the fact of filling the inner tube than the variation of the strength of the concrete employed.

3.3. Concrete-steel contribution ratio (CSCR)

The effect of the location of the type of concrete and the thick steel tube in the cross-sectional configuration are also studied in this work by means of an analysis of the mechanical contribution of the different components obtained from the experimental results.

For this purpose, a new parameter, established by the authors in a previous work [24], is utilized. Following the basis commonly used in the analysis of CFST columns, a mechanical ratio defined as the concrete-steel contribution ratio (CSCR) is employed. It is worth to note that all these specimens have the same length but not the same slenderness since it changes with the variation in the cross-sectional properties.

Thus, the CSCR is calculated as the ratio between the maximum load achieved by the CFDST (N_u) and the maximum load measured for the corresponding CFST column ($N_{u, CFST}$), given that the predictable improved mechanical response of a CFDST column with respect to

its corresponding CFST column resides in the extra inner steel tube. Therefore, for the same area of steel placed in the cross-section, a value less than unity means that the new configuration of steel tubes thicknesses combined with the infill of the inner tube does not improve the load bearing capacity of the original CFST of reference.

$$CSCR = \frac{N_u}{N_{u,CFST}} \qquad (1)$$

This parameter helps to quantify the trend observed previously through the load-deflection curves and the calculated values are shown in Table 4 and in Fig. 9.

Series 3: NSC in the outer ring

All the values calculated for the CSCR ratio are less than unity which proves that there is no combination able to improve the load bearing capacity of the CFST of reference. The specimens with configuration thick-thin present higher maximum loads than the thin-thick ones and the positive effect of the concrete infill in the inner core is more noticeable, being the double-tube column NR18, with a CSCR ratio of 0.98, the specimen whose maximum load more approximates the one of the CFST3.

Series 4: UHSC in the outer ring

The influence of the location of the thick steel tube is less clear for Series 4 than for Series 3, but still significant. Therefore, although the influence of the UHSC outer ring is evident and the maximum loads increase, the combination thick-thin shows clearly higher bearing capacity, contrarily to what observed in the CFDST columns under axial loads [24], where the UHSC outer ring dominates the overall mechanical response and the configuration of steel tubes barely had influence.

It is worth mentioning that the CSCR of the double-skin column NR22 (thick-thin) is near to unity (0.91), which means that it is possible to obtain practically the same bearing capacity with a column with less self-weight. However, this fact was more evident for the

corresponding double-skin column under axial load [24] and also notable for the double-skin specimen of the configuration thin-thick.

3.4. Inner concrete contribution ratio (ICCR)

The variation in the loading capacity of a double-skin CFDST column when its inner steel tube is filled with concrete (double-tube) is evaluated by means of the inner concrete contribution ratio (ICCR).

According to previous work published by the authors [24], it was calculated as the relation between the maximum load registered for the double-tube CFDST column and that showed during the test by the corresponding double-skin column so that a value more than unity indicates that filling the inner tube with concrete is beneficial.

$$ICCR = \frac{N_{u,CFDST,double-tube}}{N_{u,CFDST,double-skin}} \tag{2}$$

In Table 4 and Fig. 10 the numerical and graphical results are respectively shown.

Series 3: NSC in the outer ring

For Series 3, the values of the ICCR are slightly higher than for Series 4, which implies that filling the inner steel tube with concrete is more efficient for CFDST columns with NSC in the outer ring. This result was expected since the same trend was observed for the corresponding axially loaded members [24].

Regarding the cross-sectional configuration of steel tubes thicknesses, the ICCR values observed for the thin-thick columns are very similar to those obtained for the thick-thin configuration, which corroborates the fact that the steel tube thicknesses ratio limits the influence of the concrete infill.

Series 4: UHSC in the outer ring

For Series 4, the values of ICCR obtained for the combination thick-thin are slightly higher as shown in Fig. 10 and Table 4.

With respect to the influence of the inner core concrete infill, the ICCR values are very similar for both types of concrete grades, which confirms the trend explained in the previous section. For the thin-thick series both specimens have a value of 1.03 and for the thick-thin series the values are 1.05 and 1.06 for the column NR23 and the column NR24 respectively. The concrete grade has minor effect in the mechanical response of the double-tube columns with UHSC outer ring, being the steel tube configuration the dominant factor.

4. STUDY AND DISCUSSION OF EUROCODE 4

The experimental results from the tests executed in this campaign were compared to the maximum loads calculated according to the design method included in EN 1994-1-1 in its Clause 6.7.3 [8] for composite members.

Besides, it is worth to note that, for the aim of comparing, all the specimens tested are considered in this analysis although Eurocode 4 Part 1-1 [8] provisions are still limited to concrete grades up to 50 MPa.

Thus, according to Clause 6.7.3.6 of EC4-1-1 [8], the following expression based on the interaction curve shown in Fig. 11 has to be satisfied:

$$\frac{M_{Ed}}{M_{pl,N,Rd}} \leq \alpha_M \qquad (3)$$

where M_{Ed} is the maximum bending moment within the column length, α_M is a non-dimensional coefficient ($\alpha_M = 0.9$ for S355 steel) and $M_{pl,N,Rd}$ is the plastic bending resistance of the section obtained from the interaction curve M-N taking into account the normal force applied and the initial eccentricity of 50 mm considered in the experiments.

According to Eurocode 4 Part 1-1 [8], in the member verification, the second-order effects can be taken into account within the column length by means of a factor k which multiplies the greatest first order bending moment. This factor is given by:

15

$$k = \frac{\beta}{1 - \frac{N_{Ed}}{N_{cr,eff}}} \qquad (4)$$

where $N_{cr,eff}$ is the critical normal force ($\pi^2 EI_{eff}/L^2$) for the relevant axis taking into account the effective flexural stiffness considering the effective length as the column length; and β is an equivalent moment factor given by:

$$\beta = 0.66 + 0.44r \ but \ \beta \geq 0.44 \qquad (5)$$

where r is the ratio between the end moments from first order or second order global analysis. In this case, for a uniform moment distribution, r=1 and, therefore, β=1.1.

The results obtained by this method are summarized in Table 3 (EC4 $N_{b,Rd}$) together with the error calculated with respect to the experimental values. As can be seen in Fig. 12, there is not a common trend for both series in terms of the steel tube thicknesses configuration. However, it can be noticed a clear shift to the unsafe side in Series 3 (NSC in the outer ring), which could be due to the manner proposed by Eurocode 4 Part 1-1 [8] to compute the flexural stiffness taking into account the second order effects. In general, when EC4 predictions are compared with test data, a slight tendency to produce unsafe results (mean error 0.98) is observed, with a maximum error inside the ±15% boundaries.

In view of all the exposed above, it can be stated that further tests, both numerical and experimental, would be needed for evaluating the actual accuracy of EC4 method for CFDST columns taking into account the employment of ultra-high strength concrete.

5. SUMMARY AND CONCLUSIONS

This paper comprises the analysis of the experimental results obtained for a series of slender concrete-filled dual steel tubular columns tested under eccentric loads where two types of concrete, normal and ultra-high strength concrete, were considered. In the campaign, two types of CFDST columns were studied: double-skin and double-tube columns. The

mechanical responses were analysed and also compared with previous results obtained for axially loaded columns. Besides, comparisons with predictions given by Eurocode 4 were included.

The following conclusions can be drawn based on the experimental results:

- Similar trend was observed in the response of all the eccentrically loaded CFDST columns in terms of load-deflection. Contrarily to axially loaded columns, none of the columns improved the load bearing capacity of the corresponding CFST column of reference.

- Due to the crucial role that the cross-sectional area of steel working in tension has on the general behavior of these columns, the influence of the steel tube configuration is clearly detected, as opposed to axially loaded CFDST columns.

- Filling the inner steel tube with concrete, NSC or UHSC, has more influence in specimens with NSC in the outer ring (higher ICCR values).

- In general, the use of UHSC as concrete infill on CFDST is not worthy since second order effects in slender columns neglect any possible improvement of the bearing capacity.

- Considering the limited cases of this work, it can be initially inferred that the method in EC4 Part 1-1 provides slightly unsafe results for estimating the buckling resistance of CFDST columns, but further tests are recommended.

ACKNOWLEDGEMENTS

REFERENCES

[1] Portoles JM, Serra E, Romero ML. Influence of ultra-high strength infill in slender concrete-filled steel tubular columns. Journal of constructional steel research 2013; 86:107-114.

[2] Zhao, XL, Grzebieta, R. Strength and ductility of concrete filled double skin (SHS inner and SHS outer) tubes. Thin-Walled Structures 2002; 40, 199-213.

[3] Zhao XL, Han L. Double skin composite construction. Progress in structural engineering and materials 2006; 8 (3) :93-102

[4] Han, LH, Tao, Z, Huang, H, Zhao, XL. Concrete-filled double skin (SHS outer and CHS inner) steel tubular beam-columns. Thin-Walled Structures 2004; 42, 1329-1355.

[5] Elchalakani M, Zhao XL, Grzebieta R. Tests on concrete filled double-skin (CHS outer and SHS inner) composite short columns under axial compression. Thin-walled structures 2002; 40 (5):415-441.

[6] Tao, Z, Han, LH, Zhao, XL. Behaviour of concrete-filled double skin (CHS inner and CHS outer) steel tubular stub columns and beam-columns. Journal of Constructional Steel Research 2004; 60, 1129-1158.

[7] Uenaka, K., Kitoh, H. y Sonoda, K. 2010. Concrete filled double skin circular stub columns under compression. Thin-Walled Structures, 48, 19-24.

[8] CEN. EN 1994-1-1, Eurocode 4: Design of composite steel and concrete structures. Part 1-1: General rules and rules for buildings. Brussels, Belgium: Comité Européen de Normalisation; 2004

[9] Liew JYR, Xiong DX. Experimental investigation on tubular columns infilled with ultra-high strength concrete. Tubular Structures XIII. Boca Raton: Crc Press-Taylor & Francis Group. 2011; 637-645.

[10] Essopjee Y, Dundu M. Performance of concrete-filled double-skin circular tubes in compression. Composite Structures 2015; 133: 1276-1283.

[11] Wan CY, Zha X-X. Nonlinear analysis and design of concrete-filled dual steel tubular columns under axial loading. Steel and Composite Structures 2016; 20(3): 571-597.

[12] Rangan B, Joyce M. Strength of eccentrically loaded slender steel tubular columns filled with high-strength concrete. ACI Structural Journal 1992; 89(6): 676–681.

[13] Han LH. Tests on concrete filled steel tubular columns with high slenderness ratio. Advances in Structural Engineering 2000; 3(4): 337–344.

[14] Yu Q, Tao Z, Wu YX. Experimental behaviour of high performance concrete-filled steel tubular columns. Thin-Walled Structures 2008; 46: 362–370.

[15] Lue D, Liu J, Yen T. Experimental study on rectangular CFT columns with high-strength concrete. Journal of Constructional Steel Research 2007; 63(1): 37–44.

[16] Tao Z, Han L, Wang D. Experimental behaviour of concrete-filled stiffened thin-walled steel tubular columns. Thin-Walled Structures 2007; 45(5): 517–527.

[17] Portoles JM, Romero ML, Bonet JL, Filippou FC. Experimental study of high strength concrete-filled circular tubular columns under eccentric loading. Journal of Constructional Steel Research 2011; 67(4):623-633.

[18] Kilpatrick AE, Rangan BV. Tests on high-strength concrete-filled steel tubular columns. ACI Structural Journal 1999; 96(2): 268–75.

[19] Zeghiche J, Chaoui K. An experimental behaviour of concrete-filled steel tubular columns. Journal of Constructional Steel Research 2005; 61(1): 53–66.

[20] Wang YC. Tests on slender composite columns. Journal of Constructional Steel Research 1999; 49(1): 25–41.

[21] Hernández-Figueirido D, Romero ML, Bonet JL, Montalvá JM. Ultimate capacity of rectangular concrete-filled steel tubular columns under unequal load eccentricities, Journal of Constructional Steel Research 2012; 68:107–117.

[22] Hernández-Figueirido D, Romero ML, Bonet, JL, Montalvá JM. Influence of Slenderness on High-Strength Rectangular Concrete-Filled Tubular Columns with Axial Load and Nonconstant Bending Moment, Journal of Structural Engineering. 2012; 138(12): 1436–1445.

[23] Romero ML, Espinos A, Portolés JM, Hospitaler A, Ibañez C. Slender double-tube ultra-high strength concrete-filled tubular columns under ambient temperature and fire. Engineering Structures 2015; 99: 536–545.

[24] Romero ML, Ibañez C, Espinos A, Portolés JM, Hospitaler A. Influence of ultra-high strength concrete on circular concrete-filed dual steel columns. Structures 2017; 9: 13-20.

[25] Espinós A, Romero M, Serra E, Hospitaler A. Circular and square slender concrete-filled tubular columns under large eccentricities and fire. Journal of Constructional Steel Research 2015; 110: 90-100.
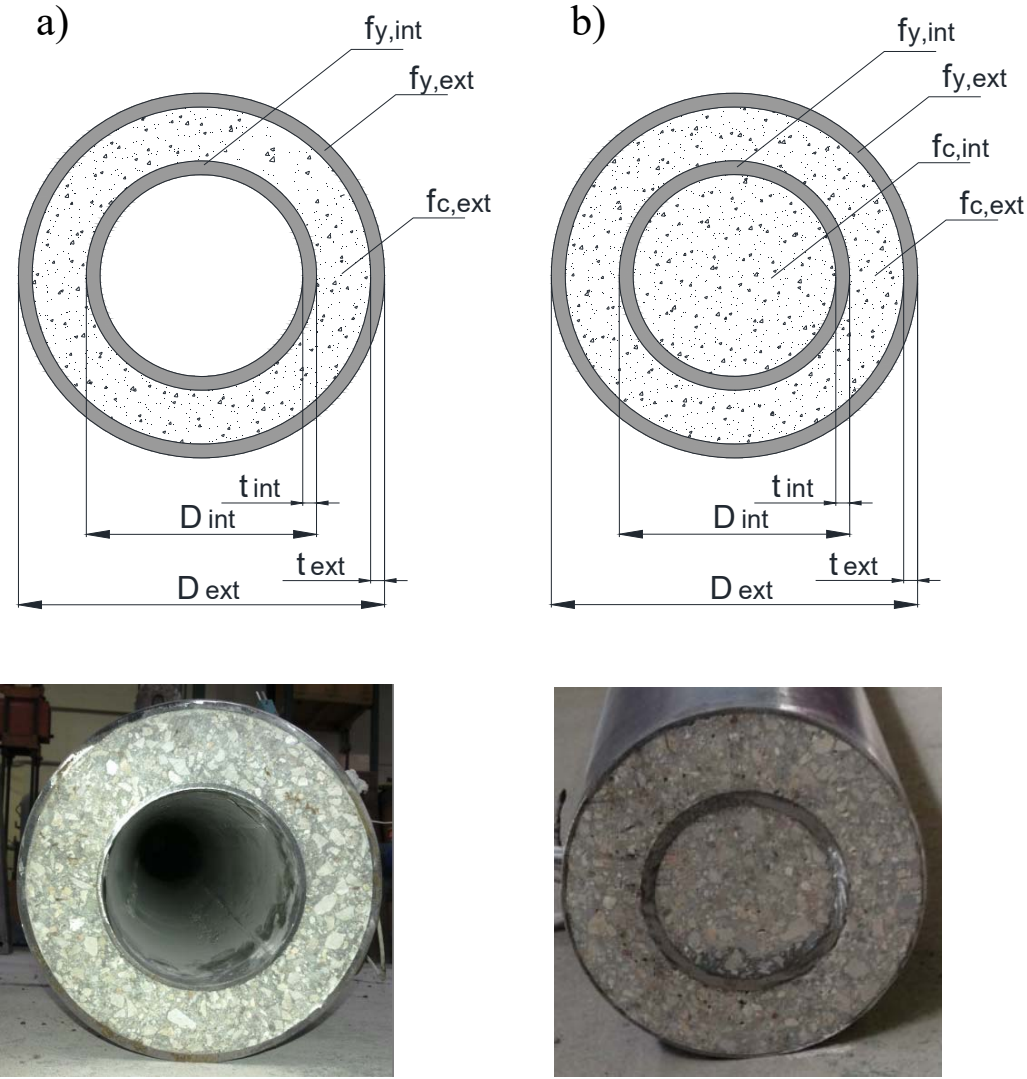
Fig. 1. CFDST sections: a) Double-skin b) Double-tube
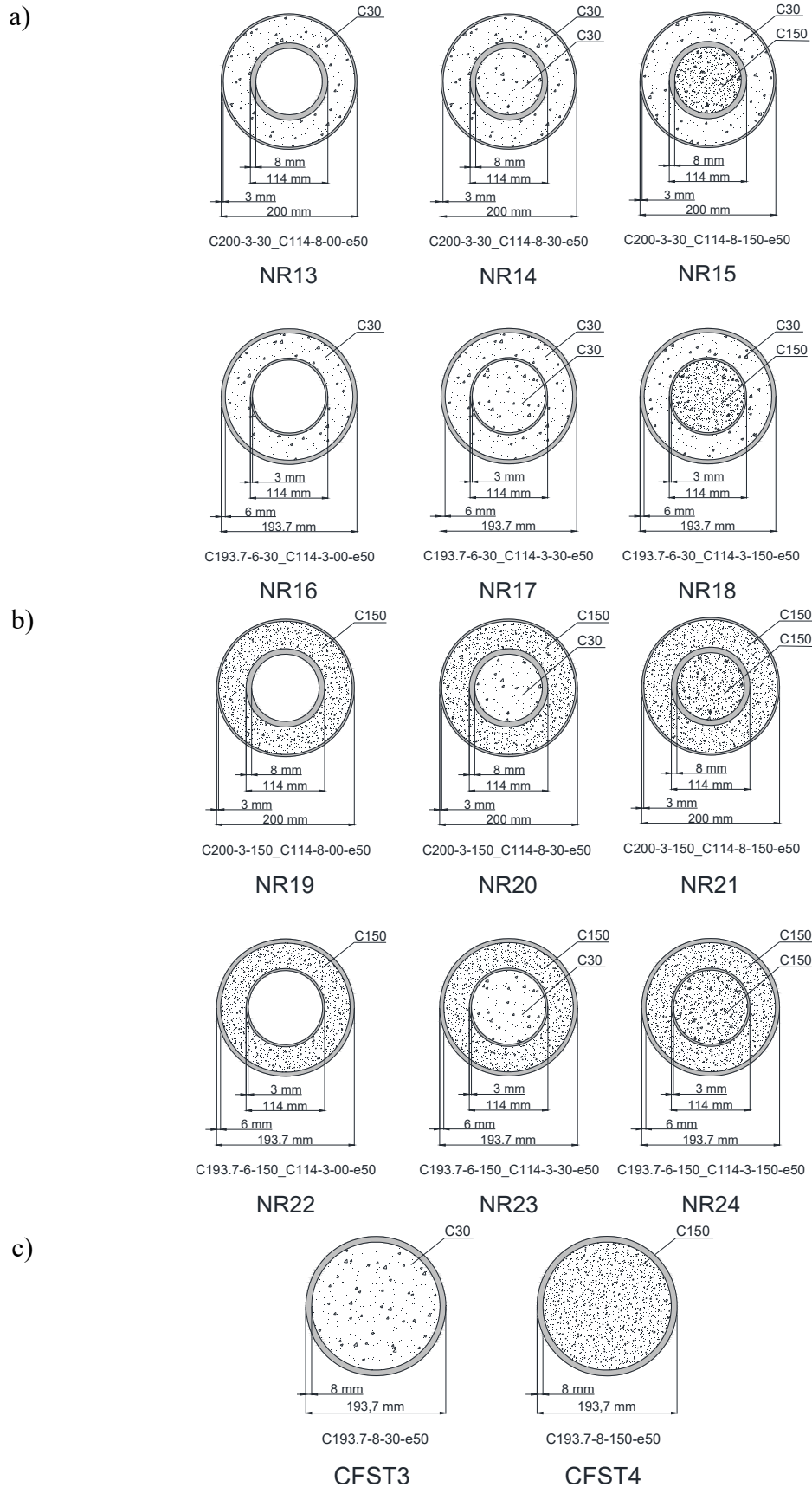
Fig. 2. Sections tested under eccentric loads: a) Series 3 b) Series 4 c) CFST specimens

a)

b)

c)
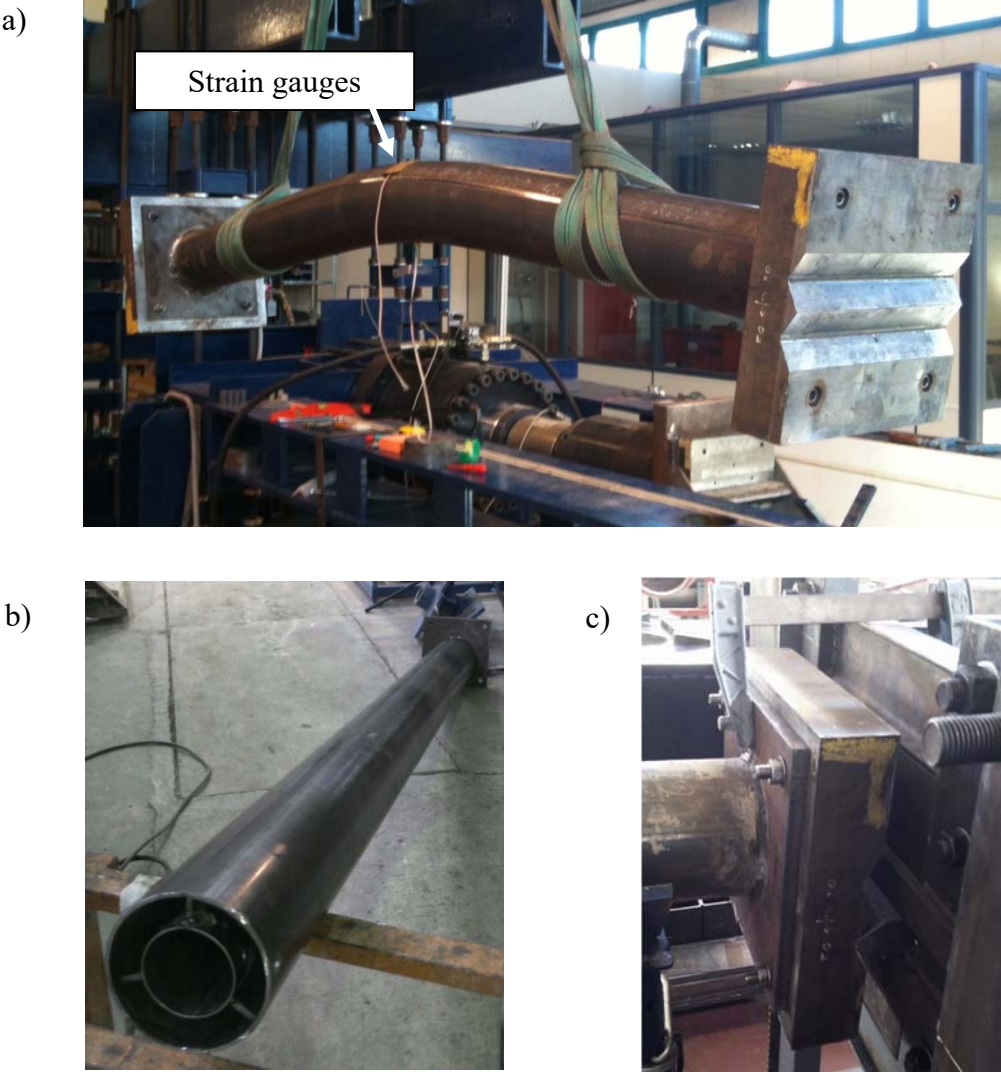
Fig. 3. Room temperature tests: a) Column after test b) Cross-section detail c) Test set-up
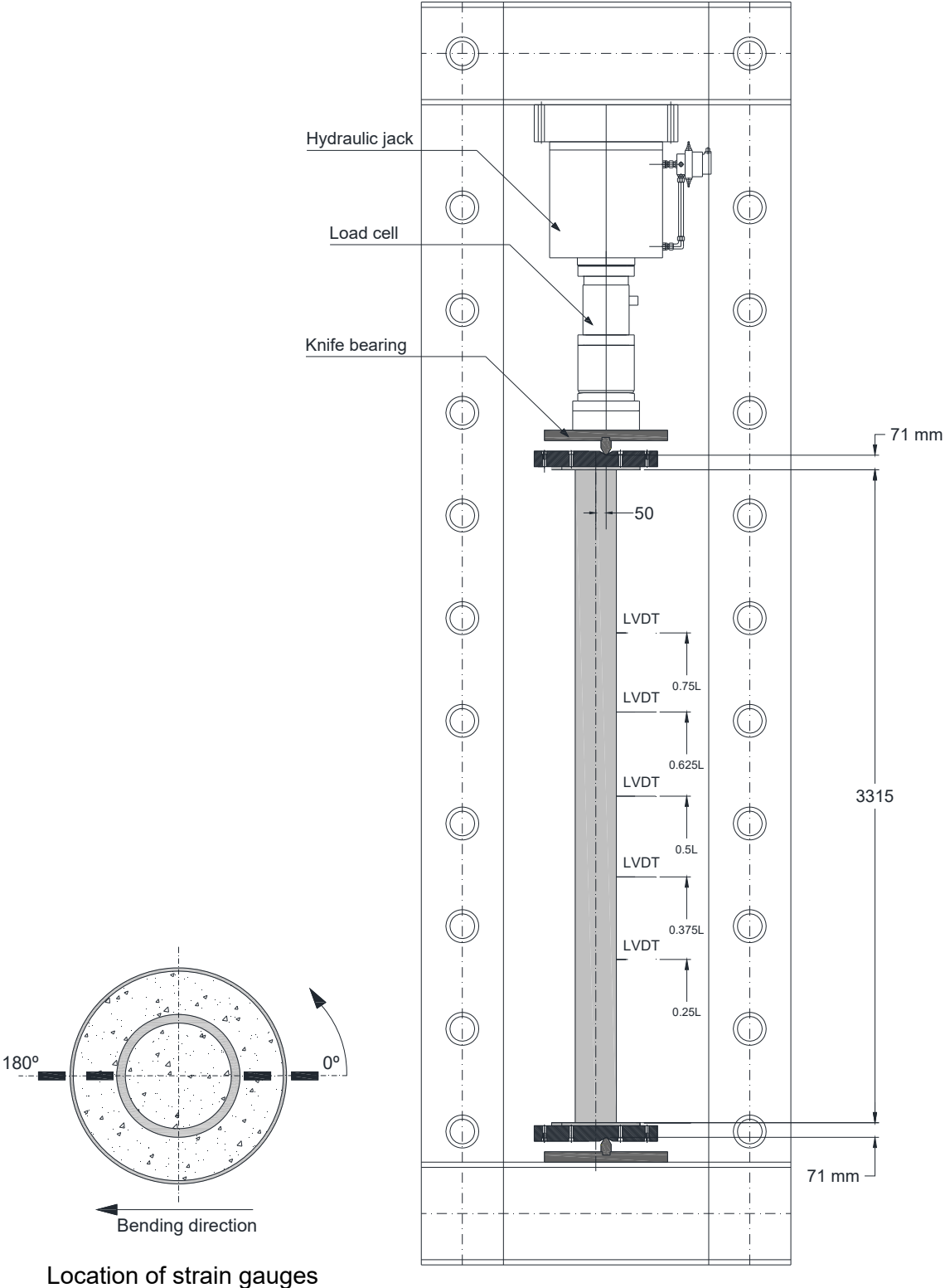
Fig. 4. Schematic view of the test set-up
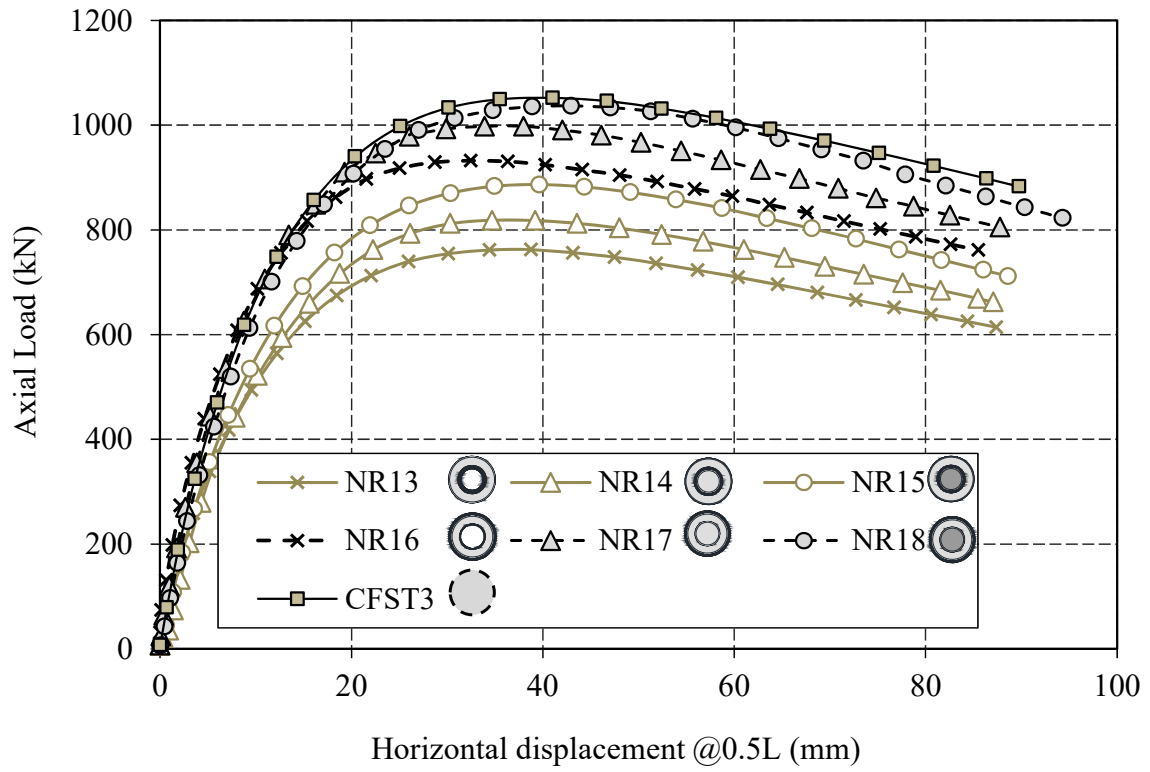
Fig. 5. Axial load versus mid-span displacement in Series 3
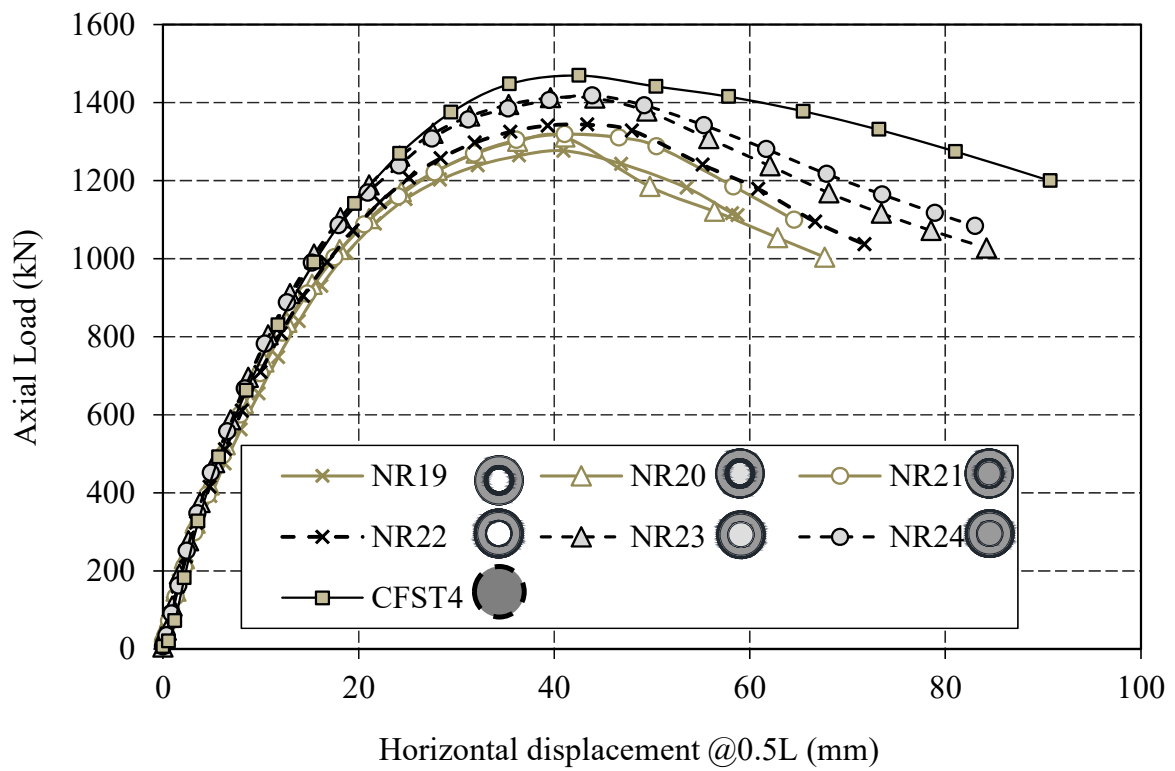
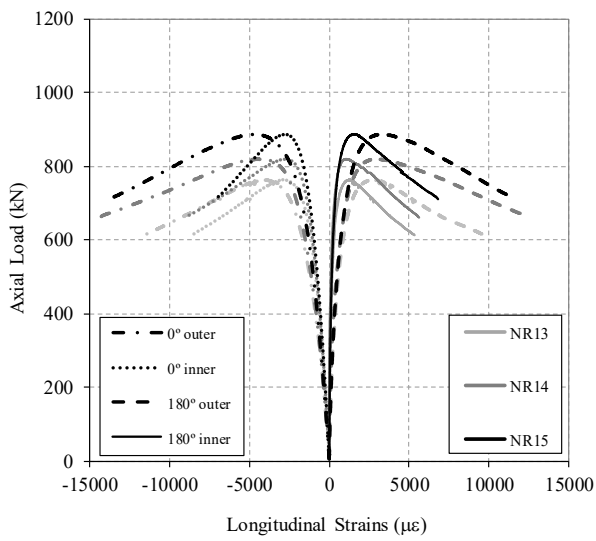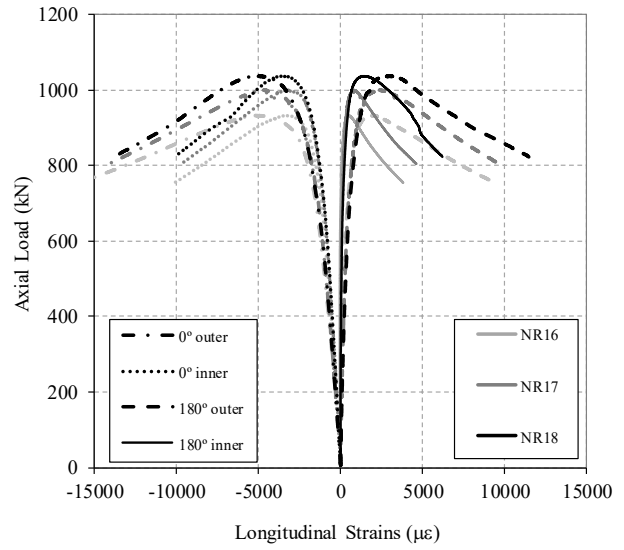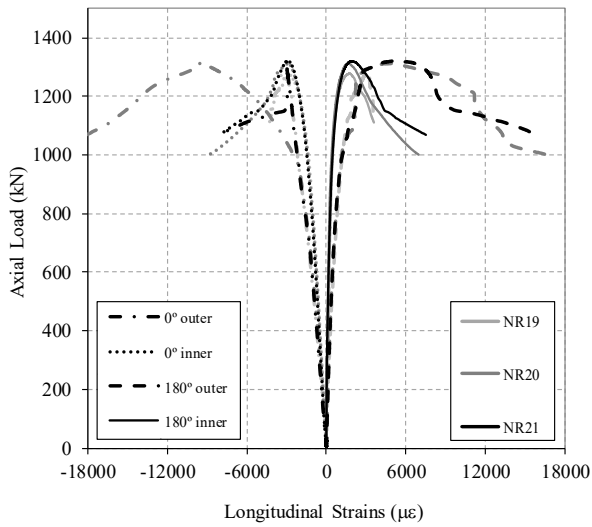Fig. 6. Axial load versus mid-span displacement in Series 4
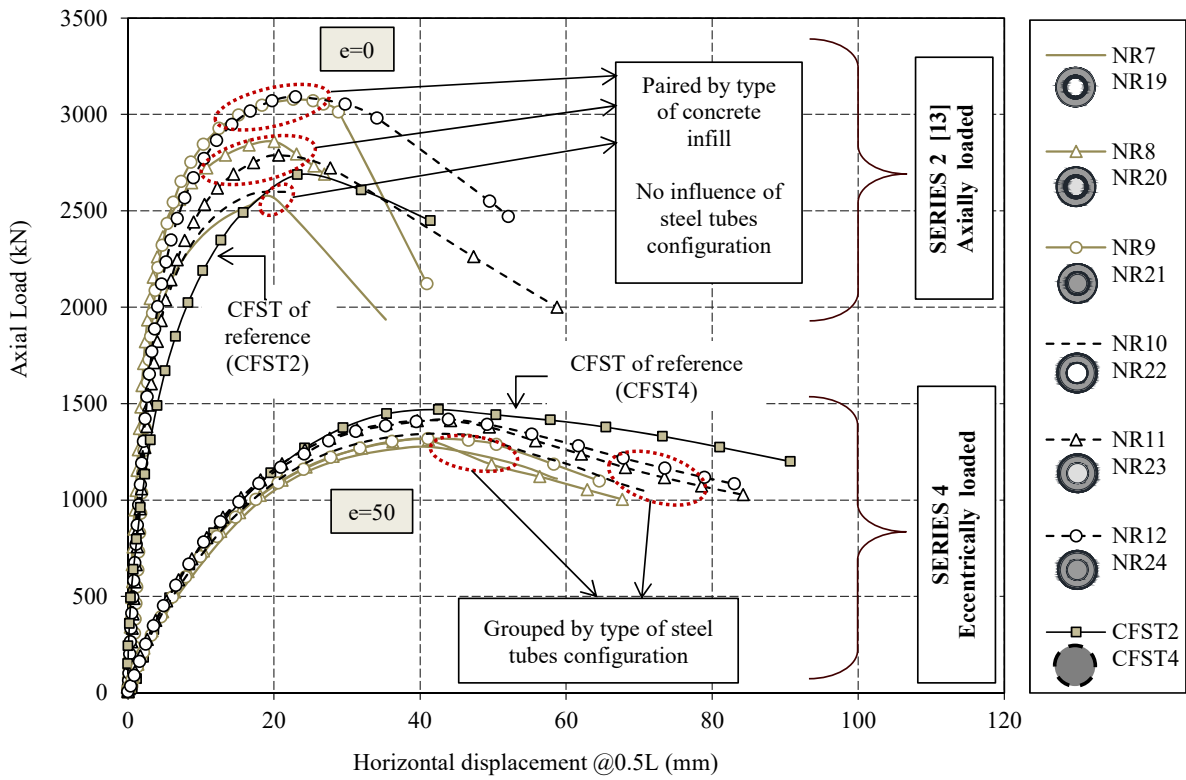
Fig. 7. Comparison of Series 4 with Series 2 from [24] (UHSC in the outer ring)

a)   Series 3, thin-thick

b)   Series 3, thick-thin

c)   Series 4, thin-thick
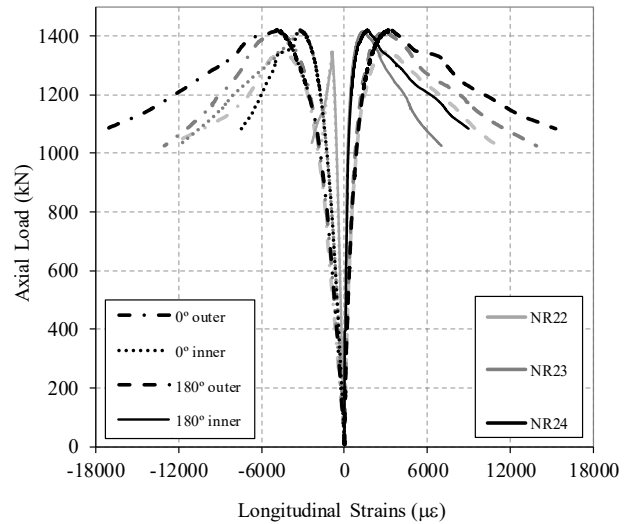
d)   Series 4, thick-thin

Fig. 8. Axial force versus longitudinal strains, ε_L at 0° and 180°
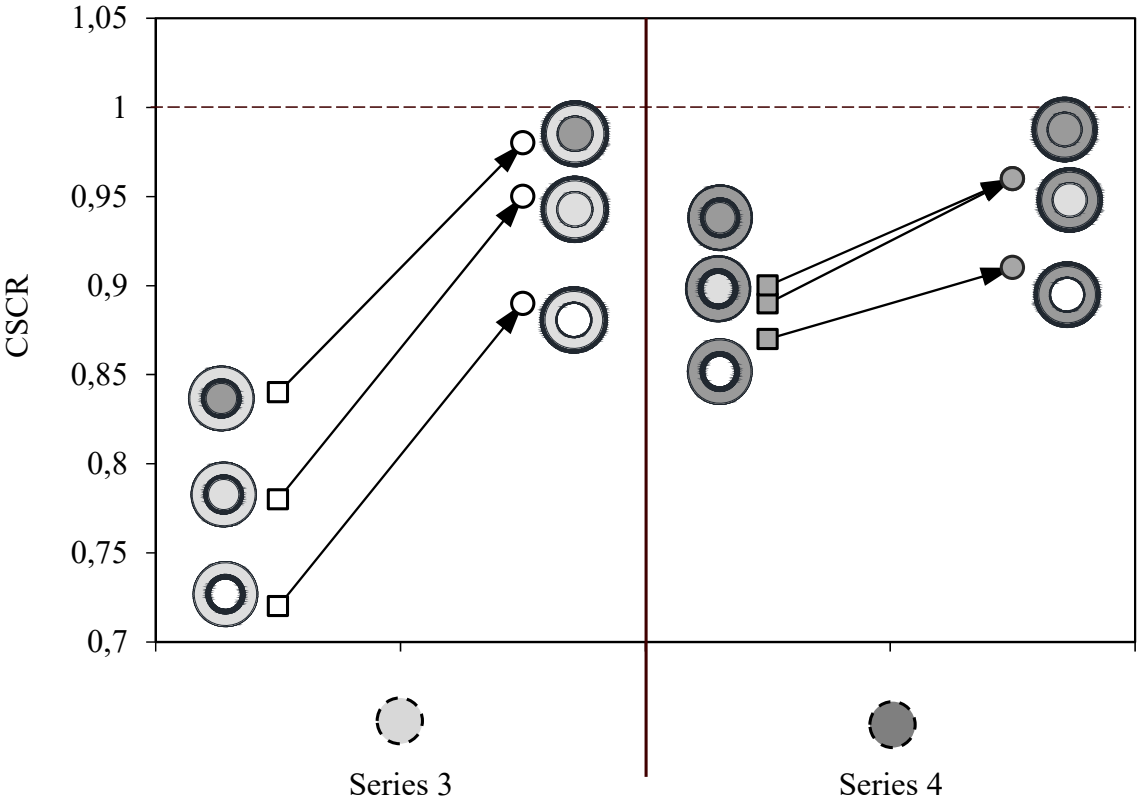
Fig. 9. Concrete-Steel contribution ratio (CSCR)
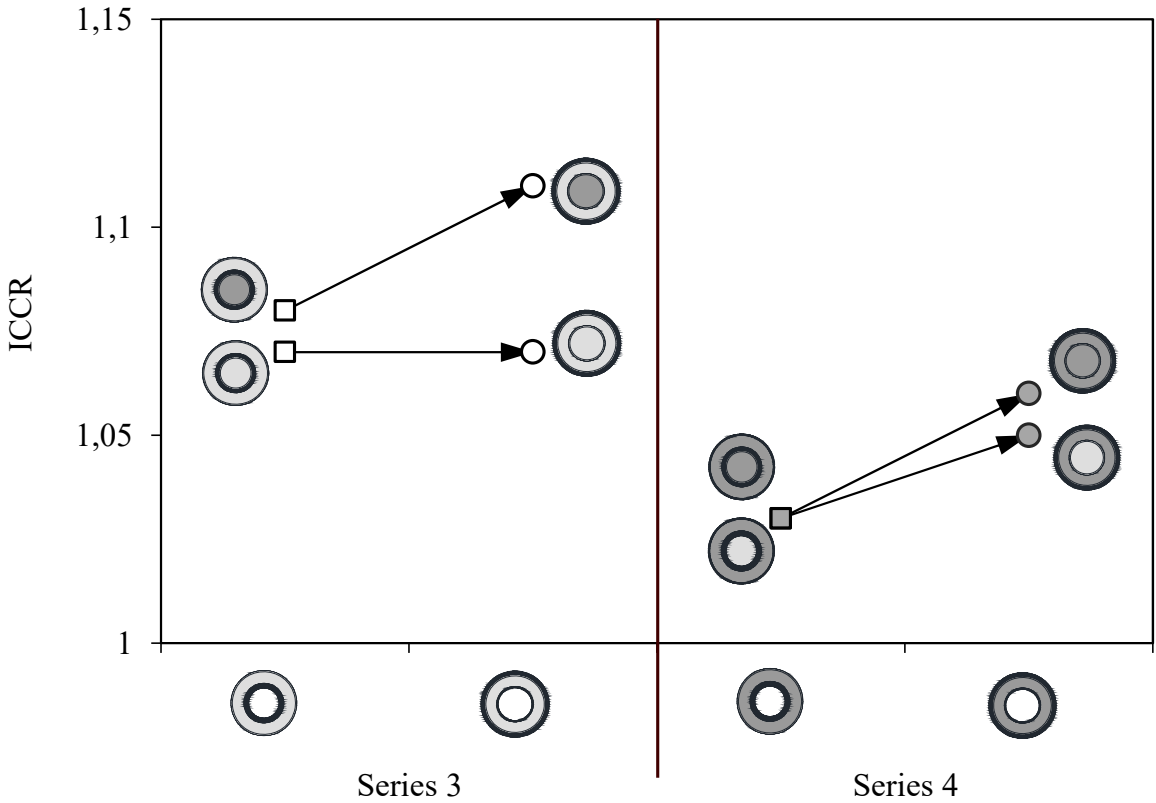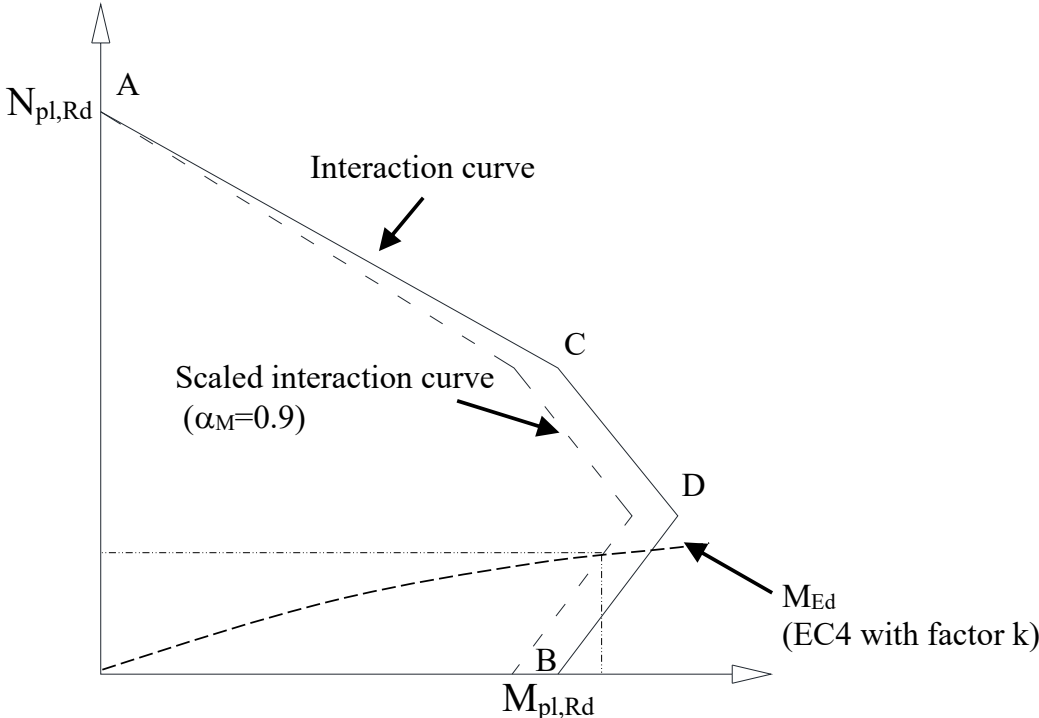
Fig. 10. Inner concrete contribution ratio (ICCR)

Fig. 11. Simplified interaction curve according to EC4, clause 6.7.3.2 [8]
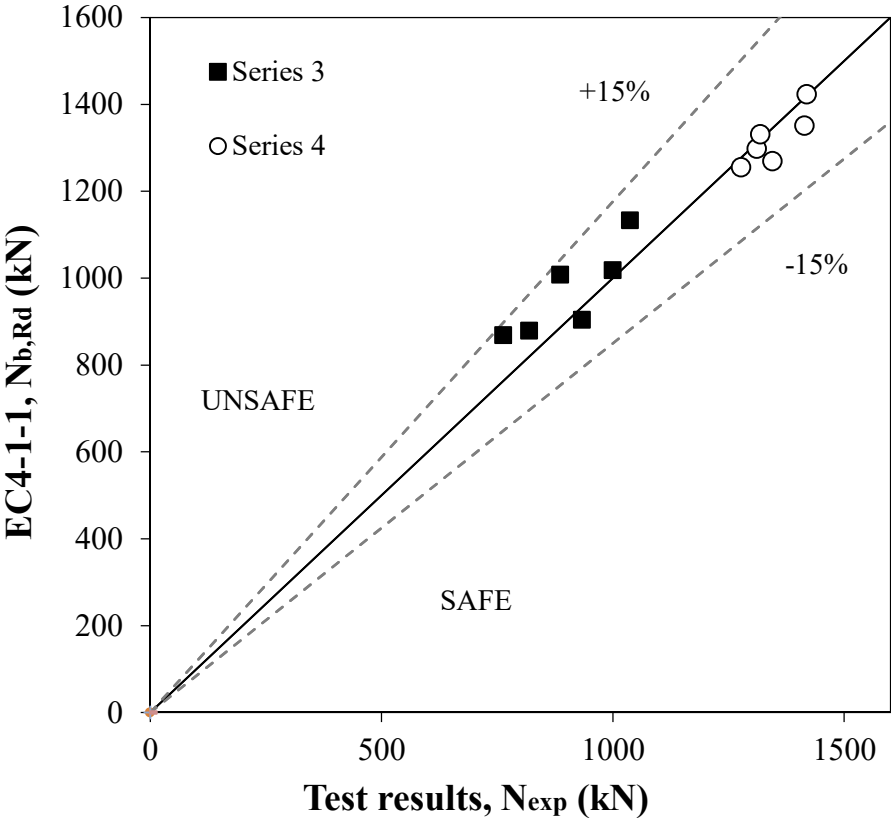
Fig. 12. Comparison between calculated buckling load (EC4) and test load

Table 1.   Details of the column specimens and test results

| ID | Column specimen | $\bar{\lambda}$ | Outer Tube | | | | | Inner Tube | | | |
			D_{ext} (mm)	t_{ext} (mm)	$f_{y,ext}$ (MPa)	$f_{c,ext}$ (MPa)	D_{int} (mm)	t_{int} (mm)	$f_{y,int}$ (MPa)	$f_{c,int}$ (MPa)
Series 3											
NR13	C200-3-30-C114-8-00-e50	0.81	200	3	318	45	114.3	8	435	0
NR14	C200-3-30-C114-8-30-e50	0.84	200	3	318	40	114.3	8	435	40
NR15	C200-3-30-C114-8-150-e50	0.97	200	3	318	55	114.3	8	435	135
NR16	C193.7-6-30-C114-3-00-e50	0.75	193.7	6	401	43	114.3	3	248	0
NR17	C193.7-6-30-C114-3-30-e50	0.79	193.7	6	401	42	114.3	3	248	42
NR18	C193.7-6-30-C114-3-150-e50	0.91	193.7	6	401	43	114.3	3	248	146
Series 4											
NR19	C200-3-150-C114-8-00-e50	1.05	200	3	400	137	114.3	8	439	0
NR20	C200-3-150-C114-8-30-e50	1.08	200	3	395	143	114.3	8	439	41
NR21	C200-3-150-C114-8-150-e50	1.15	200	3	400	143	114.3	8	439	141
NR22	C193.7-6-150-C114-3-00-e50	0.91	193.7	6	390	140	114.3	3	325	0
NR23	C193.7-6-150-C114-3-30-e50	0.95	193.7	6	390	148	114.3	3	325	45
NR24	C193.7-6-150-C114-3-150-e50	1.04	193.7	6	390	149	114.3	3	325	149
CFST specimens											
CFST3	C193.7-8-30-e50	0.8	193.7	8	441	41				
CFST4	C193.7-8-150-e50	1.03	193.7	8	433	149				

t=thickness   D=diameter   BC= pinned-pinned

Table 2.   Mix proportions

Type of infill	30	150
Cement (kg/m^3)	375	800
Water (l/m^3)	225	150
Sand (kg/m^3)	778	800
Gravel 4–7 mm (kg/m^3)	651	630
Gravel 7–12 mm (kg/m^3)	304	-
Silica fume (kg/m^3)	-	120
Super-plasticizer (kg/m^3)	-	26.3

Table 3.   Experimental and EC4 method results

ID	Column specimen	Experimental	EC4	$\xi=N_u/N_{b,Rd}$
		N_u (kN)	$N_{b,Rd}$ (kN)	
Series 3				
NR13	C200-3-30-C114-8-00-e50	763	869	0.88
NR14	C200-3-30-C114-8-30-e50	819	879	0.93
NR15	C200-3-30-C114-8-150-e50	886	1008	0.88
NR16	C193.7-6-30-C114-3-00-e50	933	904	1.03
NR17	C193.7-6-30-C114-3-30-e50	1000	1018	0.98
NR18	C193.7-6-30-C114-3-150-e50	1037	1133	0.92
Series 4				
NR19	C200-3-150-C114-8-00-e50	1277	1255	1.02
NR20	C200-3-150-C114-8-30-e50	1311	1298	1.01
NR21	C200-3-150-C114-8-150-e50	1319	1331	0.99
NR22	C193.7-6-150-C114-3-00-e50	1345	1269	1.06
NR23	C193.7-6-150-C114-3-30-e50	1414	1351	1.05
NR24	C193.7-6-150-C114-3-150-e50	1419	1423	1.00
			Mean	0.98
			Standard deviation	0.06
CFST specimens				
CFST3	C193.7-8-30-e50	1053	1201	
CFST4	C193.7-8-150-e50	1473	1659	

Table 4.   Concrete-steel contribution ratio and concrete contribution ratio

ID	Column specimen	CFST column	CSCR	Double-skin column	ICCR
Series 3					
NR13	C200-3-30-C114-8-00-e50		0.72		---
NR14	C200-3-30-C114-8-30-e50	C194-8-30-00-e50	0.78	NR13 C200-3-30-C114-8-00-e50	**1.07**
NR15	C200-3-30-C114-8-150-e50		0.84		**1.08**
NR16	C193.7-6-30-C114-3-00-e50		0.89		---
NR17	C193.7-6-30-C114-3-30-e50		0.95	NR16 C200-6-30-C114-3-00-e50	**1.07**
NR18	C193.7-6-30-C114-3-150-e50		0.98		**1.11**
Series 4					
NR19	C200-3-150-C114-8-00-e50		0.87		---
NR20	C200-3-150-C114-8-30-e50	C194-8-150-00-e50	0.89	NR19 C200-3-150-C114-8-00-e50	**1.03**
NR21	C200-3-150-C114-8-150-e50		0.90		**1.03**
NR22	C193.7-6-150-C114-3-00-e50		0.91		---
NR23	C193.7-6-150-C114-3-30-e50		0.96	NR22 C200-6-150-C114-3-00-e50	**1.05**
NR24	C193.7-6-150-C114-3-150-e50		0.96		**1.06**

CSCR= concrete-steel contribution ratio, eq. (1)
ICCR= inner concrete contribution ratio, eq. (2)

LIST OF FIGURE CAPTIONS

Fig. 1.   CFDST sections: a) Double-skin b) Double-tube

Fig. 2.   Sections tested under eccentric loads: a) Series 3 b) Series 4 c) CFST specimens

Fig. 3.   Room temperature tests: a) Column after test b) Cross-section detail c) Test set-up

Fig. 4.   Schematic view of the test set-up

Fig. 5.   Axial load versus mid-span displacement in Series 3

Fig. 6.   Axial load versus mid-span displacement in Series 4

Fig. 7.   Comparison of Series 4 with Series 2 from [24] (UHSC in the outer ring)

Fig. 8.   Axial force versus longitudinal strains, ε_L at 0° and 180°

Fig. 9.   Concrete-Steel contribution ratio (CSCR)

Fig. 10.   Inner concrete contribution ratio (ICCR)

Fig. 11.   Simplified interaction curve according to EC4, clause 6.7.3.2 [8]

Fig. 12.   Comparison between calculated buckling load (EC4) and test load

LIST OF TABLE CAPTIONS

Table 1. Details of the column specimens and test results

Table 2. Mix proportions

Table 3. Experimental and EC4 method results

Table 4. Concrete-steel contribution ratio and concrete contribution ratio